

Same-Sign Tetra-Leptons from Type II Seesaw

Eung Jin Chun and Pankaj Sharma

Korea Institute for Advanced Study, Seoul 130-722, Korea

Abstract

The type II seesaw mechanism introduces a hypercharged Higgs triplet to explain the observed neutrino masses and mixing. Among three triplet components, the doubly charged Higgs boson can be the lightest and decay mainly to same-sign di-leptons. Furthermore, the heavier singly charged or neutral Higgs boson produces a doubly charged Higgs boson through its fast gauge decay. This leads to a novel signature of same-sign tetra-leptons resulting from a pair production of same-sign doubly charged Higgs bosons caused by the nearly degenerate neutral scalar mixing which can be sizable for an appropriate choice of the model parameters. After studying production cross-sections for the same-sign tetra-lepton signal in the parameter space of the mass splitting among triplet components and the triplet vacuum expectation value, we provide a LHC analysis of the same-sign tetra-lepton signal for a benchmark point chosen to maximize the event number.

1 Introduction

The origin of neutrino masses and mixing can be attributed to a new “Higgs triplet” which can couple to Higgs and lepton doublets and thus generate neutrino mass terms once it develops nontrivial vacuum expectation value (called the “type II seesaw” mechanism) [1]. One of the distinctive features of the type II seesaw model is the presence of a doubly charged Higgs boson which can be cleanly probed at collider experiments [2]–[7]. This allows an exciting possibility of discovering the neutrino mass pattern at colliders by observing the lepton flavor structure of the doubly charged Higgs boson decay to same-sign charged lepton pairs [8]. Because of such a nice property, extensive studies at the LHC have been performed in the literature [9]–[20].

In this paper, we investigate a novel signature of same-sign tetra-leptons allowed in some parameter space of the type II seesaw model that has not been studied so far. The mass splitting among three Higgs triplet components (neutral, singly and doubly charged) is controlled by a single coupling between the triplet and the usual doublet Higgs bosons and its sign determines whether the lightest component is a doubly charged or neutral one. When the mass splitting is sizable and the doubly charged Higgs boson is the lightest, the electroweak gauge interaction allows a fast decay of the neutral or singly charged component of the Higgs triplet into the lighter singly or doubly charged component. Therefore, pair-produced Higgs triplet components can end up with a pair of same-sign doubly charged Higgs bosons leading to same-sign tetra-leptons if their leptonic Yukawa coupling is larger than the ratio of the triplet and doublet Higgs vacuum expectation values.

An essential feature of a $l^\pm l^\pm l^\pm l^\pm$ signal is that it occurs through the mixing between two nearly degenerate neutral scalars. In the limit of vanishing triplet vacuum expectation value (VEV), lepton number is conserved and thus there appear only $l^+ l^+ l^- l^-$ final states coming from the production of $H^{++} H^{--}$ pairs [17, 20]. A non-vanishing triplet VEV arises due to the coupling between the Higgs triplet and doublet which explicitly breaks lepton number in the Lagrangian. This term also induces the mass splitting between two real degrees of freedom in the neutral triplet scalar. While this mass splitting becomes very small for a small triplet VEV, the neutral triplet decay rate is also suppressed by a small mass difference among the triplet components. It turns out that there exists an optimal choice of the model parameters for which the sizes of the neutral scalar mass splitting and decay rate become comparable and the doubly charged Higgs boson decays mainly to same-sign di-lepton to maximize the production cross-section of the $4l^\pm$

signal.

The same-sign tetra-lepton final state, which is almost background free, provides an excellent new channel to test the model and probe sizes of the Higgs triplet vacuum expectation value and the mass splitting among the Higgs triplet components at the LHC.¹

In the next section, we will introduce the type II seesaw model following the notation of Ref. [8]. In Section III, the branching ratios of the Higgs triplet components will be studied in a parameter space of the mass splitting and the triplet vacuum expectation value. Then, in Section IV analyzed are the same-sign tetra-lepton signals at the LHC with two centre-of-mass energies of $\sqrt{s} = 8$ TeV (LHC8) and $\sqrt{s} = 14$ TeV (LHC14) for the doubly charged Higgs boson mass 400 GeV taking a benchmark point in the two dimensional parameter space which maximizes the the neutral boson mixing effect. We conclude in Section V.

2 The Type II Seesaw Model

When the Higgs sector of the Standard Model is extended to have a $Y = 2$ complex $SU(2)_L$ scalar triplet Δ in addition to a SM-Higgs doublet Φ , the gauge-invariant Lagrangian is written as

$$\mathcal{L} = (D_\mu \Phi)^\dagger (D^\mu \Phi) + \text{Tr} (D_\mu \Delta)^\dagger (D^\mu \Delta) - \mathcal{L}_Y - V(\Phi, \Delta)$$

where the leptonic part of the Lagrangian required to generate neutrino masses is

$$\mathcal{L}_Y = f_{\alpha\beta} L_\alpha^T C i \tau_2 \Delta L_\beta + \text{H.c.} \quad (1)$$

and the scalar potential is

$$\begin{aligned} V(\Phi, \Delta) &= m^2 \Phi^\dagger \Phi + \lambda_1 (\Phi^\dagger \Phi)^2 + M^2 \text{Tr}(\Delta^\dagger \Delta) \\ &+ \lambda_2 [\text{Tr}(\Delta^\dagger \Delta)]^2 + \lambda_3 \text{Det}(\Delta^\dagger \Delta) + \lambda_4 (\Phi^\dagger \Phi) \text{Tr}(\Delta^\dagger \Delta) \\ &+ \lambda_5 (\Phi^\dagger \tau_i \Phi) \text{Tr}(\Delta^\dagger \tau_i \Delta) + \left[\frac{1}{\sqrt{2}} \mu (\Phi^T i \tau_2 \Delta \Phi) + \text{H.c.} \right]. \end{aligned} \quad (2)$$

Here used is the 2×2 matrix representation of Δ :

$$\Delta = \begin{pmatrix} \Delta^+/\sqrt{2} & \Delta^{++} \\ \Delta^0 & -\Delta^+/\sqrt{2} \end{pmatrix}. \quad (3)$$

¹Let us note that same-sign four leptons can also appear among others in the cascade decays of supersymmetric particles if R-parity violating supersymmetry is assumed [21].

Upon the electroweak symmetry breaking with $\langle\Phi^0\rangle = v_0/\sqrt{2}$, the μ term in Eq. (2) gives rise to the vacuum expectation value of the triplet $\langle\Delta^0\rangle = v_\Delta/\sqrt{2}$ where $v_\Delta \approx \mu v_0^2/\sqrt{2}M^2$. We will assume μ is real positive without loss of generality.

After the electroweak symmetry breaking, there are seven physical massive scalar eigenstates denoted by $H^{\pm,\pm}$, H^\pm , H^0 , A^0 , h^0 . Under the condition that $|\xi| \ll 1$ where $\xi \equiv v_\Delta/v_0$, the first five states are mainly from the triplet scalar and the last from the doublet scalar. For the neutral pseudoscalar and charged scalar parts,

$$\begin{aligned}\phi_I^0 &= G^0 - 2\xi A^0, & \phi^+ &= G^+ + \sqrt{2}\xi H^+ \\ \Delta_I^0 &= A^0 + 2\xi G^0, & \Delta^+ &= H^+ - \sqrt{2}\xi G^+\end{aligned}\quad (4)$$

where G^0 and G^+ are the Goldstone modes, and for the neutral scalar part,

$$\begin{aligned}\phi_R^0 &= h^0 - a\xi H^0, \\ \Delta_R^0 &= H^0 + a\xi h^0\end{aligned}\quad (5)$$

where $a = 2 + 4(4\lambda_1 - \lambda_4 - \lambda_5)M_W^2/g^2(M_{H^0}^2 - M_{h^0}^2)$. The masses of the Higgs bosons are

$$\begin{aligned}M_{H^{\pm\pm}}^2 &= M^2 + 2\frac{\lambda_4 - \lambda_5}{g^2}M_W^2 \\ M_{H^\pm}^2 &= M_{H^{\pm\pm}}^2 + 2\frac{\lambda_5}{g^2}M_W^2 \\ M_{H^0, A^0}^2 &= M_{H^\pm}^2 + 2\frac{\lambda_5}{g^2}M_W^2.\end{aligned}\quad (6)$$

The mass of h^0 is given by $m_{h^0}^2 = 4\lambda_1 v_\Phi^2$ as usual.

Eq. (6) tells us that the mass splitting among triplet scalars can be approximated as

$$\Delta M \approx \frac{\lambda_5 M_W^2}{g^2 M} < M_W. \quad (7)$$

Furthermore, depending upon the sign of the coupling λ_5 , there are two mass hierarchies among the triplet components: $M_{H^{\pm\pm}} > M_{H^\pm} > M_{H^0/A^0}$ for $\lambda_5 < 0$; or $M_{H^{\pm\pm}} < M_{H^\pm} < M_{H^0/A^0}$ for $\lambda_5 > 0$. In this work, we focus on the latter scenario, where the doubly charged scalar $H^{\pm\pm}$ is the lightest so that it decays only to $l_\alpha^\pm l_\beta^\pm$ or $W^\pm W^\pm$ whose coupling constants are proportional to $f_{\alpha\beta}$ or ξ , respectively. On the other hand, H^0/A^0 (H^\pm) decays mainly to $H^\pm W^{\mp*}$ ($H^{\pm\pm} W^{\mp*}$) unless the mass splitting ΔM is negligibly small. For more details, see, e.g., Ref. [8].

An important quantity for a $4l^\pm$ signal is the mass splitting δM_{HA} between H^0 and A^0 which is much smaller than the mass difference ΔM between different triplet components. The μ term

in Eq. (2), which is lepton number violating, generates not only the triplet VEV:

$$v_\Delta = \frac{\mu v_0^2}{\sqrt{2}M_{H^0}^2}, \quad (8)$$

but also the mass splitting between the heavy neutral scalars, $\delta M_{HA} \equiv M_{H^0} - M_{A^0}$:

$$\delta M_{HA} = 2M_{H^0} \frac{v_\Delta^2}{v_0^2} \frac{M_{H^0}^2}{M_{H^0}^2 - m_{h^0}^2}. \quad (9)$$

As will be shown later, δM_{HA} can be comparable to the total decay rate of the neutral scalars, Γ_{H^0/A^0} , for a preferable choice of v_Δ , which enhances the same-sign tetra lepton signal.

Given the leptonic Yukawa term (1), a non-zero triplet vacuum expectation value $\langle \Delta^0 \rangle$ gives rise to the neutrino mass matrix:

$$M_{\alpha\beta}^\nu = \sqrt{2}f_{\alpha\beta}v_\Delta \equiv U_{\alpha k}U_{\beta k}m_k e^{i\phi_k} \quad (10)$$

where U is the neutrino mixing matrix with Majorana phases $e^{i\phi_k}$ factored out, and m_k are the neutrino mass eigenvalues. The mixing matrix U is described by three angles denoted by θ_{12} , θ_{23} , and θ_{13} , and one Dirac phase δ . The three angles and two mass-squared differences Δm_{21}^2 and Δm_{31}^2 are fairly well measured by various neutrino experiments [22]. As the sign of Δm_{31}^2 is not yet known, two neutrino mass hierarchies are allowed. One is the normal hierarchy (NH) with $m_3 > m_2 > m_1$ and the other is the inverted hierarchy (IH) with $m_2 > m_1 > m_3$. Thus, the neutrino mass matrix (10) can be fully reconstructed after some assumptions on values of the CP phases, δ and ϕ_k , and one neutrino mass, say m_1 (m_3) for NH (IH) which can be as small as zero.

For the collider analysis, we will take benchmark points for each neutrino mass hierarchy assuming $m_1(m_3) = 0$ for NH (IH) and vanishing CP phases. Taking the best fit values [22] given by $\Delta m_{21}^2 = 7.62 \times 10^{-5} \text{ eV}^2$, $\Delta m_{31}^2 = 2.53 \times 10^{-3} (-2.40) \text{ eV}^2$, $\sin^2 \theta_{12} = 0.320$, $\sin^2 \theta_{23} = 0.49(0.53)$ and $\sin^2 \theta_{13} = 0.026(0.027)$ for NH (IH), we get the following neutrino mass matrix in the eV unit:

$$M^\nu = \begin{pmatrix} 0.00403 & 0.00816 & 0.00259 \\ 0.00816 & 0.0264 & 0.0215 \\ 0.00259 & 0.0215 & 0.0286 \end{pmatrix} \text{ for NH} \quad (11)$$

and

$$M^\nu = \begin{pmatrix} 0.0479 & -0.00557 & -0.00573 \\ -0.00557 & 0.0239 & -0.0240 \\ -0.00573 & -0.0240 & 0.02693 \end{pmatrix} \text{ for IH.} \quad (12)$$

Thus, the leptonic Yukawa coupling f can be obtained from Eq. (10) given the triplet vacuum expectation value v_Δ . To get an estimate of the overall size of f it is useful to remember $f v_\Delta \sim 10^{-2}$ eV derived from a rough relation of $f v_\Delta \sim m_k$. Recall that the neutrino mass matrices (11,12) tell about the flavor-dependent branching fractions of $H^{\pm\pm}$ and thus observation of $ee/e\mu/\mu\mu$ final states at the LHC will be able to determine which neutrino mass pattern is right [8].

3 Phase diagrams for branching fractions of Triplet decay

Apart from the parameters set by the neutrino data in the coupling f , there are two more free parameters in the type II seesaw model: the triplet mass splitting ΔM and the triplet vacuum expectation value v_Δ . Depending on these, the triplet components have different decay properties. In Table. 1, we show the possible decay channels for the triplet scalars for the case where H^{++} is the lightest. The decays to the lepton and quark/di-boson final states are due to the Yukawa coupling f and a mixture of the doublet and triplet Higgs controlled by $\xi = v_\Delta/v_0$, respectively. On the other hand, the final states with off-shell W is due to the usual $SU(2)$ gauge interaction which dominates if allowed kinematically.

H^0	A^0	H^+	H^{++}
$\rightarrow t\bar{t}$	$\rightarrow t\bar{t}$	$\rightarrow t\bar{b}$	$\rightarrow \ell^+\ell^+$
$\rightarrow b\bar{b}$	$\rightarrow b\bar{b}$	$\rightarrow \ell^+\nu$	$\rightarrow W^+W^+$
$\rightarrow \nu\bar{\nu}$	$\rightarrow \nu\bar{\nu}$	$\rightarrow W^+Z$	
$\rightarrow ZZ$	$\rightarrow Zh^0$	$\rightarrow W^+h^0$	
$\rightarrow h^0h^0$	$\rightarrow H^\pm W^\mp^*$	$\rightarrow H^{++}W^{-*}$	
$\rightarrow H^\pm W^\mp^*$			

Table 1: Possible decay channels for the triplet Higgs bosons for $\lambda_5 > 0$.

Summing over all the lepton final states in the triplet decays, the flavor structure of neutrino mass matrix does not matter as the total leptonic decay rate is proportional to $\sum_k m_k^2$. Keeping this parameter to be $(0.1 \text{ eV})^2$, we calculate the branching fractions (BFs) for each scalar depending on two parameters: ΔM and v_Δ . In Fig. 1, we show phase diagrams for H^+ and H^{++} decays in the plane of ΔM and v_Δ . In the left panel, the brown, the gray and the

purple regions show the branching fractions for the decays $H^+ \rightarrow H^{++}W^{-*}$, $H^+ \rightarrow \ell^+\nu$ and $H^+ \rightarrow \{t\bar{b}, W^+Z, W^+h\}$, respectively. In the right panel, the brown and the gray regions show the branching fractions for the decays $H^{++} \rightarrow W^+W^+$ and $H^{++} \rightarrow \ell^+\ell^+$ respectively. In both panels, the dark-colored regions denote the parameter space where the branching fraction is greater than 99% and the light-colored regions denote the parameter space where the branching fraction is between 50%-99%.

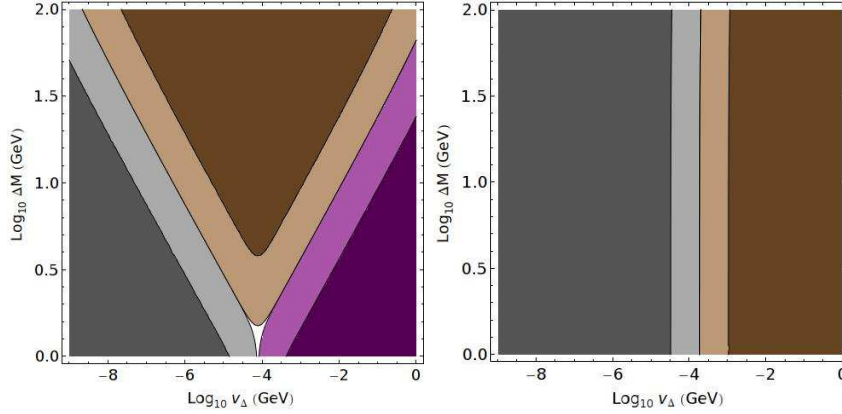


Figure 1: Phase diagrams for H^+ (left) and H^{++} (right) decays in the type II seesaw model for $\lambda_5 > 0$ with $M_H^{++} = 300$ GeV. The dark-colored regions denote the branching fraction larger than 99%.

As it can be seen from Fig. 1, the leptonic decay of H^+ ($H^+ \rightarrow \ell^+\nu$) is dominant for small values of $v_{\Delta} < 0.1$ MeV (corresponding to $|f| > |\xi|$). For low values of v_{Δ} and ΔM , this BF is always greater than 0.99. However, for moderate mass splitting $\Delta M > 5$ GeV, the decay $H^+ \rightarrow H^{++}W^{-*}$ start becoming dominant at $v_{\Delta} = 0.1$ MeV. For slightly larger value of ΔM at around 10-20 GeV, there is much larger parameter space opening up for this decay. Hence, we can see that for moderate v_{Δ} (around 1 keV-10 MeV), large mass splitting is allowed for the branching fraction larger than 99%. On the other hand, for large v_{Δ} and low mass splitting, rest of the decays viz., ($H^+ \rightarrow t\bar{b}, W^+Z, W^+h$) have appreciable contributions and thus $\text{BF}(H^+ \rightarrow H^{++}W^{-*})$ goes down.

For the $H^{\pm\pm}$ decays, we see that for $v_{\Delta} < 0.1$ MeV, it is completely dominated by leptonic decay i.e., $H^{\pm\pm} \rightarrow \ell^{\pm}\ell^{\pm}$ while for $v_{\Delta} > 1$ MeV, it is dominated by the decay to two W^{\pm} s. These BFs are completely independent of the mass splitting ΔM as is obvious from that the $H^{\pm\pm}$ is the lightest.

Similarly, in Fig. 2, we show phase diagrams for H^0 and A^0 decays in the plane of ΔM and v_Δ . In the left panel, the brown, the gray and the purple regions show the BF's for the decays $H^0 \rightarrow \nu\bar{\nu}$, $H^0 \rightarrow H^+W^{-*}$, and $H^0 \rightarrow \{t\bar{t}, b\bar{b}, ZZ, h^0h^0\}$ respectively. In the right panel, the brown, the gray and the purple regions show the BF's for the decays $A^0 \rightarrow \nu\bar{\nu}$, $A^0 \rightarrow H^+W^{-*}$, and $A^0 \rightarrow \{t\bar{t}, b\bar{b}, Zh^0\}$ respectively. In both panels, the dark-colored regions denote the parameter space where BF is between 49%-50% and the light-colored regions denote the parameter space where the BF is between 20%-49%.

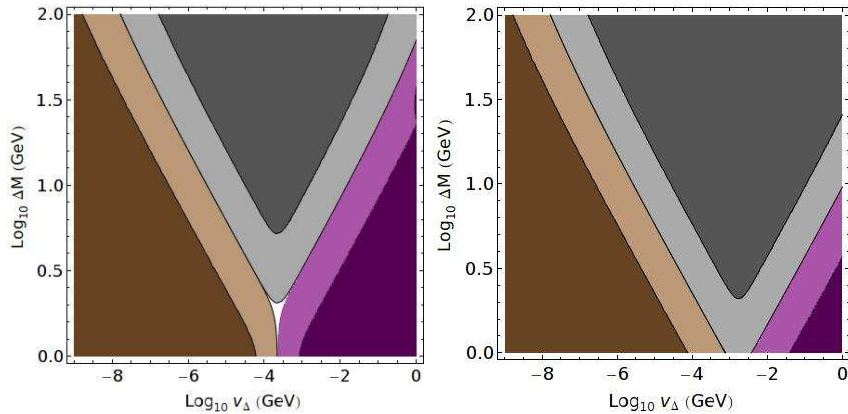


Figure 2: Phase diagrams for H^0 (left) and A^0 (right) decays in the type II seesaw model for $\lambda_5 > 0$ with $M_H^{++} = 300$ GeV. The dark-colored regions denote the branching fraction in the range of 49%-50%.

4 Same-Sign Tetra-Leptons at the LHC

A remarkable feature of the Type II seesaw model would be the observation of doubly charged Higgs bosons $H^{\pm\pm}$ at the TeV scale. Production of such scalars has been extensively studied in processes $q\bar{q} \rightarrow Z^*/\gamma^* \rightarrow H^{++}H^{--}$ [7, 10, 15, 17] and $q'\bar{q} \rightarrow W^* \rightarrow H^{\pm\pm}H^\mp$ [9]. The pair production mechanism leads to four lepton signals including a pair of same-sign di-leptons with opposite charges, or tri-lepton signals which are relatively clean and thus studied by many authors. In this section, we study a new possibility of probing the type II seesaw model at the LHC through a distinctive signal of four same-sign leptons which are either positively or negatively charged. The processes which contribute to such a signal are as follows:

1. $q'\bar{q} \rightarrow W^* \rightarrow H^\pm H^0/A^0$

proceeded by $H^\pm \rightarrow H^{\pm\pm}W^\mp$ and $H^0/A^0 \rightarrow H^\pm W^\mp \rightarrow H^{\pm\pm}W^\mp W^\mp$;

2. $q\bar{q} \rightarrow Z^* \rightarrow H^0 A^0$

proceeded by $H^0/A^0 \rightarrow H^\pm W^\mp \rightarrow H^{\pm\pm}W^\mp W^\mp$.

The above mentioned production cross-sections of triplet scalars only depend on the scalar masses because the interactions are due to the triplet gauge couplings. The cross-section for process 2 is the largest among the three. Out of all the triplet pairs produced in the above three processes, only some fraction of them eventually give same-sign $H^{\pm\pm}$ pairs whose production is controlled by the neutral scalar mixing parameter as will be discussed below.

We further assume leptonic decays of $H^{\pm\pm}$ to be dominant, which is allowed for a large part of parameter space (with $|f| > |\xi|$) as can be seen from Fig. 1. The processes 1 and 2 give a signal which contains $4\ell^\pm + X$ where X contains jets and leptons coming from off-shell W s which are soft and thus hard to be detected due to a small mass gap between the triplet components.

As noted in Refs. [17, 20], the $4\ell^\pm$ final state cannot occur in the limit of lepton number conservation, that is, $\mu, v_\Delta \rightarrow 0$, due to the cancelling interference between H^0 and A^0 . However, the above processes 1 and 2 are allowed when there is a finite mass difference (9) violating lepton number. In the limit of $M_{H^0/A^0} \gg \delta M_{HA}, \Gamma_{H^0/A^0}$ as well as $\Gamma_{H^0} \simeq \Gamma_{A^0}$, one can find a simple expression for the $4\ell^\pm$ production rate following a proper treatment of the interference effect in the narrow width approximation. Note that this phenomenon occurs as H^0 and A^0 , sharing the same final states, can mix together like in the $B^0-\bar{B}^0$ system. In other words, Δ^0 can oscillate to $\Delta^{0\dagger}$ and vice versa to produce wrong sign leptons in our system. If they undergo sufficient oscillation before they decay, i.e., $\delta M_{HA} \gtrsim \Gamma_{H^0/A^0}$, the lepton number violating production of same-sign tetra-leptons becomes sizable. That is, this effect is controlled by the usual oscillation parameter x_{HA} :

$$x_{HA} \equiv \frac{\delta M_{HA}}{\Gamma_{H^0/A^0}}. \quad (13)$$

From the calculation of the H^0 - A^0 interference term in the narrow width approximation, we obtain the cross-sections for the processes 1 and 2 as follows:

$$\begin{aligned} \sigma(4\ell^\pm + 3W^\mp) &= \sigma(pp \rightarrow H^\pm H^0 + H^\pm A^0) \left[\frac{x_{HA}^2}{1 + x_{HA}^2} \right] \text{BF}(H^0/A^0 \rightarrow H^\pm W^\mp) \\ &\times [\text{BF}(H^\pm \rightarrow H^{\pm\pm} W^\mp)]^2 [\text{BF}(H^{\pm\pm} \rightarrow \ell^\pm \ell^\pm)]^2; \end{aligned} \quad (14)$$

$$\begin{aligned} \sigma(4\ell^\pm + 4W^\mp) &= \sigma(pp \rightarrow H^0 A^0) \left[\frac{2 + x_{HA}^2}{1 + x_{HA}^2} \frac{x_{HA}^2}{1 + x_{HA}^2} \right] \text{BF}(H^0 \rightarrow H^\pm W^\mp) \\ &\times \text{BF}(A^0 \rightarrow H^\pm W^\mp) [\text{BF}(H^\pm \rightarrow H^{\pm\pm} W^\mp)]^2 [\text{BF}(H^{\pm\pm} \rightarrow \ell^\pm \ell^\pm)]^2. \end{aligned} \quad (15)$$

As expected, the cross-sections vanish for $x_{HA} \rightarrow 0$ recovering the lepton number conserving limit. In the limit of $x_{HA} \gg 1$ (the maximal lepton number violation), the mixing factors become one and the $4l^\pm$ signal numbers are controlled only by the branching fractions of H^0 and A^0 . For a rough estimation of x_{HA} , let us compare δM_{HA} in Eq. (9) with the gauge decay rate of H^0/A^0 given by

$$\Gamma_{H^0/A^0} \sim \frac{G_F^2 \Delta M^5}{\pi^3}. \quad (16)$$

From this one finds that $x_{HA} \sim 1$ can be obtained with, e.g., $v_\Delta \sim 10^{-4}$ GeV and $\Delta M \sim 2$ GeV.

Since we are interested in four same-sign leptons in the final state, the cross-section for such a signal also depend on v_Δ through the decay branching fractions. These signals depend on $[\text{BF}]^5$ and $[\text{BF}]^6$, so we should look at those regions of parameter space where these BF's are maximum. To explore those regions in the $\Delta M - v_\Delta$ plane, we plot the products of BF's which occur in the evaluation of cross-sections of those signals. In Fig. 3, we show product of BF's for processes 1 (left figure) and for process 2 (right figure) in $\Delta M - v_\Delta$ plane. One can see from these figures that there are large parameter space where these products are maximum i.e., 0.5. In Fig. 4 (bottom), we show sum of cross-sections for processes 1 and 2 which can finally give same-sign tetra-leptons. The cross-sections are independent of v_Δ and steadily decreases with the rise of ΔM . In Fig. 4 (top), we show cross-sections for $\ell^\pm \ell^\pm \ell^\pm \ell^\pm$ signal at LHC8 and LHC14 in the $\Delta M - v_\Delta$ plane. The Fig. 4 (top) is obtained by superposing the Figs. 4 (bottom) and 3 and multiplying with the oscillation factor as in Eqs. (14,15). The doubly charged Higgs mass is taken to be 400 GeV. Note that the CMS experiment puts a lower bound on the doubly charged Higgs boson which decays only to charged leptons: $M_{H^{\pm\pm}} > (330 - 360)$ GeV considering the pair production only [23]. One can see from Fig. 4 that the same-sign tetra-lepton cross-section is maximized for $v_\Delta = (10^{-4} - 10^{-5})$ GeV and $\Delta M = (1 - 2)$ GeV in accordance with the rough estimate. To recapitulate the condition for large number of same-sign tetra-lepton events, one needs $x_{HA} \gtrsim 1$

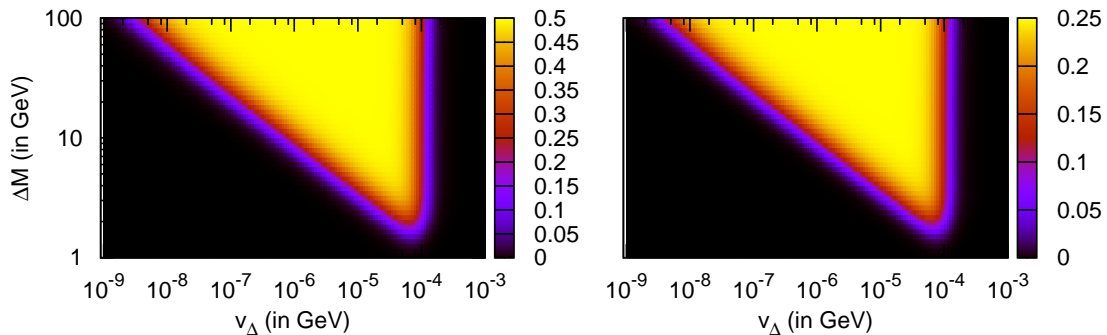


Figure 3: Product of branching fractions for processes 1 (left), and 2 (right).

enhancing the H^0 - A^0 mixing and appropriate ΔM small enough to increase the production of $H^0/A^0 H^\pm$, *etc*, but not too small to suppress the decays $H^0/A^0 \rightarrow H^\pm W^*$, *etc*, assuming of course the dominance of the leptonic decays channels of $H^{\pm\pm}$. As far as the latter condition is realized, the type II seesaw can be tested by observing the usual signals of a pair of same-sign di-leptons from $H^{++}H^{--} \rightarrow l^+l^+l^-l^-$. If the parameter region sits near the limited bright region in Fig. 4, one can look in addition for four same-sign leptons allowing to get information about v_Δ and ΔM . Furthermore, in the limit of $x_{HA} \gg 1$, the transition probability of Δ^0 to $\Delta^{0\dagger}$ is maximized to be one-half rendering the number of same-sign tetra-leptons comparable to that of a pair of same-sign di-leptons, and thus it will be more efficient to look for the same-sign tetra-lepton signals.

We remark that lepton flavor violating processes like $\mu \rightarrow ee\bar{e}$ are highly suppressed in the parameter region of our interest. For $v_\Delta \sim (10^{-4} - 10^{-5})$ GeV, the neutrino mass relation (10) requires $f_{ij} \sim (10^{-6} - 10^{-7})$, whereas one needs, for instance, $f_{11}f_{12} > 10^{-8}$ to observe the signal of $\mu \rightarrow ee\bar{e}$ in the future experiments [8].

Now let us take a benchmark point with $v_\Delta = 7 \times 10^{-5}$ GeV, $\Delta M = 1.5$ GeV and $M_{H^{\pm\pm}} = 400$ GeV which gives $\delta M_{HA} = 3.68 \times 10^{-11}$ GeV, $\Gamma_{H^0/A^0} = 3.73 \times 10^{-11}$ GeV, and thus $x_{HA}^2/(1 + x_{HA}^2) = 0.79$. In Table. 2, we show the values of pair production cross-sections relevant for our calculation at LHC8 and LHC14.

So far, we have not distinguished among flavors of charged leptons i.e., e, μ, τ in our analysis. However, we know that at the LHC, τ leptons are more difficult to identify and have large backgrounds. τ leptons can decay leptonically $\tau \rightarrow e\nu_e\bar{\nu}_\tau$ and $\tau \rightarrow \mu\nu_\mu\bar{\nu}_\tau$ with branching

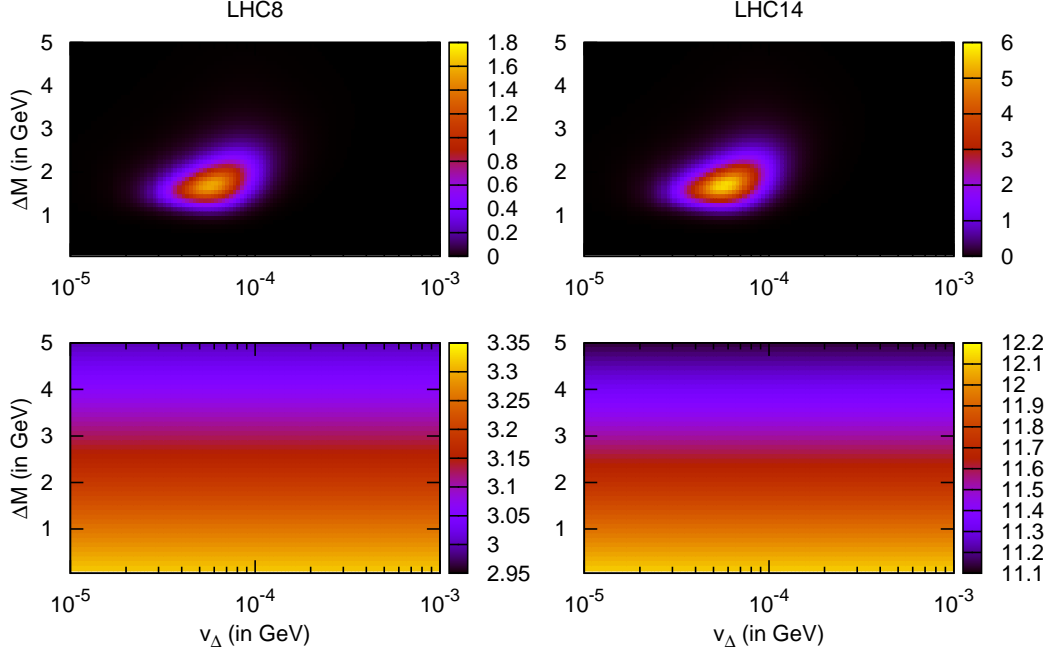


Figure 4: Bottom panels show cross-sections (in fb) for $H^\pm H^0/H^\pm A^0/H^0 A^0$ production, and top panels for same-sign tetra-lepton events. Left (right) panels are for LHC8 (LHC14).

fractions of 17% each. These e 's and μ 's are less energetic than their parent τ 's. On the other hand, decays $H^{\pm,\pm} \rightarrow e^\pm e^\pm/\mu^\pm \mu^\pm/e^\pm \mu^\pm$ are much cleaner and produce the two energetic e and μ closer to invariant mass $M_{H^{\pm,\pm}}$. For the collider analysis including lepton flavor dependence, we consider the full neutrino mass matrices calculated in Eqs. (11, 12) for the NH and IH, respectively. In the NH case, the BF of the $H^{\pm,\pm}$ decay to the e and μ final states is 32%, and thus $H^{\pm,\pm}$ decay mainly to same-sign τ pairs. Of course, the leptonic decays of these τ 's to e/μ are included in our analysis. On the other hand, for the IH case, the $H^{\pm,\pm}$ decay BF to the e and μ final states is 60% and thus we expect to have more same-sign tetra-lepton signal events compared to the NH case.

In Table 3, we show number of events before selection cuts and after selection cuts for both NH and IH at two center of mass energies 8 TeV and 14 TeV LHC. We assume 15 fb^{-1} and 100 fb^{-1} of integrated luminosities for LHC8 and LHC14 respectively.

We expect almost no background to our same-sign tetra-lepton signal. The only potential background can come from multi W production with at least four W^\pm and extra W^\mp demanding four W^\pm decaying leptonically and the rest W^\mp hadronically. In the lowest order, there is a diagram for $4W^\pm + 2W^\mp$ production whose cross-section is proportional to α_{EW}^7 . Other back-

Final State	σ/fb (8 TeV)	σ/fb (14 TeV)
$H^+ H^0$	0.761	2.931
$H^+ A^0$	0.761	2.931
$H^- H^0$	0.275	1.209
$H^- A^0$	0.275	1.209
$H^0 A^0$	1.014	4.322

Table 2: The values of cross-section for different sub-processes contributing to same-sign tetra-lepton signals for the LHC8 and LHC14. We use $\Delta M = 1.5$ GeV and $M_{H^{\pm\pm}} = 400$ GeV for LHC8 and LHC14.

ground can come from $gg \rightarrow 4W^+ + 4W^-$ which is a loop process with top- and bottom-quarks inside the loop. The cross-section for this process would be suppressed by $\alpha_S^2 \alpha_{EW}^8$ times loop-suppression factor. Thus, the background for resulting number of same-sign tetra-lepton final states is practically zero at the LHC.

Since there is negligible background, the selection criteria for the leptons are very trivial. We just need to have those cuts which are essential for detector acceptance regions. So, the basic cuts like $p_T > 20$ GeV and $|\eta| < 2.5$ for all leptons would be sufficient to detect our signal. We use CTEQ6L [24] parton distribution function (PDF) and the renormalization/factorization scale is set at $2M_{H^+}$. We use CALCHEP [25] to generate the parton level events for the relevant processes. Then, using LHEF [26] interface, we pass these parton level events to PYTHIA [27] for fragmentation and initial/final state radiations. We use PYCELL, a toy calorimeter in PYTHIA, for hadronic level simulation for finding jets using a cone algorithm. For realistic simulation, we use the following criteria for selection of events:

- There should be exactly 4 isolated leptons (e, μ) of same sign in the events,
- $p_T^\ell > 20$ GeV, $|\eta| < 2.5$ and $\Delta R(\ell_i, \ell_j) > 0.2$.
- leptons are arranged in decreasing order in p_T and are labelled as ℓ_i , ($i = 1, \dots, 4$) in that order.
- no jet should overlap with any lepton.

In Table 3 we show the total number of four same-sign lepton events before and after applying selection cuts. We list these numbers for both NH and IH scenarios for both LHC8 and LHC14

with 15 fb^{-1} and 100 fb^{-1} of integrated luminosities respectively. We find that after applying the section cuts, the total number of events are reduced by 25%. The number of events in the IH scenario is twice the number of events in NH scenario. This is due to the fact that the branching ratio $\text{BF}(H^{\pm\pm} \rightarrow ee/e\mu/\mu\mu)$ is almost twice in IH scenario relative to NH as noted before. One can see that the signal event numbers are large enough to test the type II seesaw mechanism through same-sign tetra-lepton final states.

The same-sign tetra-lepton signal for $M_{H^{++}} = 400 \text{ GeV}$ might be barely observable at LHC8 for the IH case, but the event number is too small to reconstruct its mass. On the other hand, LHC14 with 100 fb^{-1} of integrated luminosity would have large number of events to look for the doubly charged Higgs mass of $M_{H^{++}} = 400 \text{ GeV}$. Assuming that 10 signal events would be sufficient for the claim of discovery, we also find that $H^{\pm\pm}$ with mass $M_{H^{++}}$ as large as 600 GeV and 700 GeV can be probed for NH and IH scenario respectively at the LHC14 with 100 fb^{-1} of integrated luminosity.

	Pre-selection	Selection
$\ell^\pm \ell^\pm \ell^\pm \ell^\pm$ (LHC8-NH)	4	3
$\ell^\pm \ell^\pm \ell^\pm \ell^\pm$ (LHC8-IH)	9	8
$\ell^\pm \ell^\pm \ell^\pm \ell^\pm$ (LHC14-NH)	110	94
$\ell^\pm \ell^\pm \ell^\pm \ell^\pm$ (LHC14-IH)	240	210

Table 3: Number of events for same-sign tetra-lepton signals before and after selection cuts for both NH and IH scenarios at LHC8 and LHC14 with 15 fb^{-1} and 100 fb^{-1} of integrated luminosities respectively.

In Fig. 5, we plot the reconstructed $H^{\pm\pm}$ mass from the sample of selected same-sign tetra-lepton events for both NH and IH neutrino mass scenarios at LHC14 with 100 fb^{-1} integrated luminosity. The peaks in all plots correspond to $H^{\pm\pm} \rightarrow ee/e\mu/\mu\mu$ decays while the broad part (off-peak) of distribution correspond to τ decays. For IH, the number of events at the peak is about 2.5 times larger than NH and the peaks are more pronounced. One can clearly see that the doubly charged Higgs boson mass can be readily found also from the same-sign tetra-lepton signal for our benchmark point.

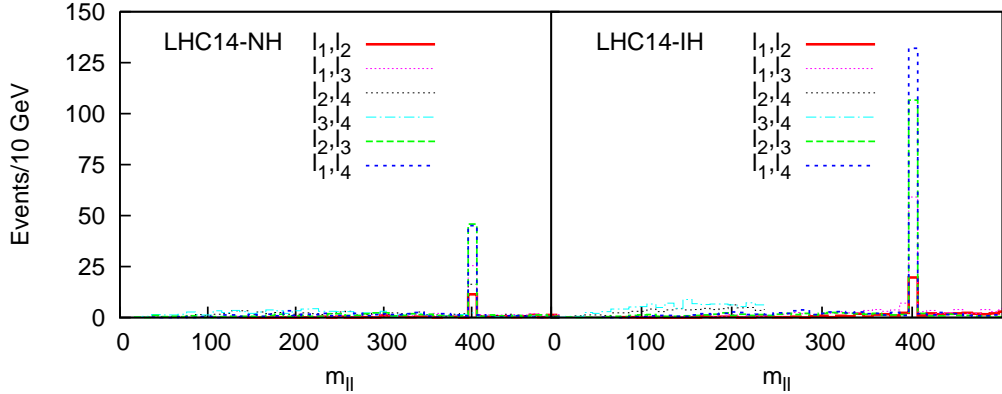


Figure 5: Invariant mass from $4\ell^\pm$ final states.

5 Conclusion

It is pointed out that a remarkable signal of same-sign tetra-lepton, $l^\pm l^\pm l^\pm l^\pm$, is allowed in the type II seesaw mechanism introducing a Higgs triplet as the origin of neutrino masses and mixing. Observability of such a signal at the LHC strongly depends on the mass splitting ΔM among the triplet components and the triplet vacuum expectation value v_Δ (or the overall size of the leptonic Yukawa coupling given by $f \sim 0.01\text{eV}/v_\Delta$). When the doubly charged component $H^{\pm\pm}$ is the lightest, larger ΔM allows more efficient gauge decay of the neutral component to the singly charged one and then to the doubly charged one. Thus, a pair production of the triplet components at colliders can end up with producing $H^{\pm\pm}H^{\pm\pm}$ whose branching fraction to same-sign tetra-leptons becomes larger for smaller v_Δ . Another crucial ingredient for increasing the $4l^\pm$ signal number is the H^0 - A^0 mixing parameter x_{HA} which becomes smaller for smaller v_Δ and larger ΔM . Therefore, there appear optimal values of the model parameters which maximize the same-sign tetra-lepton signal.

After studying such a behavior in the $\Delta M - v_\Delta$ plane, we identified a benchmark point with $\Delta M = 1.5$ GeV and $v_\Delta = 7 \times 10^{-5}$ GeV for maximized the signal numbers at the LHC. The collider analysis of a same-sign tetra-lepton signal is trivial as it is completely background free. After making the typical selection cuts to identify four same-sign leptons, we have shown that one can obtain sizable event numbers for $M_{H^{\pm\pm}} = 400$ GeV with integrated luminosity of 100 fb^{-1} at the LHC14 to reconstruct the doubly charged Higgs mass in both cases of the normal and inverted neutrino mass hierarchy. We also found that the doubly charged Higgs boson mass up to 600 GeV and 700 GeV can be probed at LHC14 for NH and IH scenarios for our benchmark

point, assuming 10 signal events for a discovery of the type II seesaw mechanism.

With accumulating data at the LHC, it is worthwhile to make a discovery or exclusion study of the type II seesaw mechanism in the full parameter space of $M_{H^{\pm\pm}}$, ΔM and v_Δ through the $l^\pm l^\pm l^\pm l^\pm$ signal as well as the conventional signal of $l^+ l^+ l^- l^-$ followed by the production of $H^{++} H^{--}$ which has been studied extensively in the literature. We leave this as future work.

Acknowledgments: We are grateful to Andrew Akeroyd and Hiroaki Sugiyama for their comments on the interference effect in the narrow width approximation. EJC was supported by the National Research Foundation of Korea (NRF) grant funded by the Korea government (MEST) (No. 20120001177).

References

- [1] M. Magg and C. Wetterich, Phys. Lett. B **94** (1980) 61; T. P. Cheng and L. -F. Li, Phys. Rev. D **22** (1980) 2860; R. N. Mohapatra and G. Senjanovic, Phys. Rev. D **23** (1981) 165.
- [2] J.F. Gunion, J. Grifols, A. Mendez, B. Kayser and F. Olness, Phys. Rev. **D40** (1989) 1546; R. Vega and D. Dicus, Nucl. Phys. **B329** (1990) 533; J.F. Gunion, R. Vega and J. Wudka, Phys. Rev. **D42** (1990) 1673;
- [3] R. Godbole, B. Mukhopadhyaya and M. Nowakowski, Phys. Lett. **B352** (1995) 388; K. Cheung, R. Phillips and A. Pilaftsis, Phys. Rev. **D51** (1995) 4731; K. Huitu, J. Maalampi, A. Pietila and M. Raidal, Nucl. Phys. **B487** (1997) 27.
- [4] T.G. Rizzo, Phys. Rev. **D45** (1992) 42; N. Lepore, B. Thorndyke, H. Nadeau and D. London, Phys. Rev. **D50** (1994) 2031.
- [5] B. Dion *et. al.*, Phys. Rev. **D59** (1999) 075006; A. Datta and A. Raychaudhuri, Phys. Rev. **D62** (2000) 055002.
- [6] E. Ma, M. Raidal and U. Sarkar, Phys. Rev. Lett. **85** (2000) 3769; Nucl. Phys. **B615** (2001) 313.
- [7] M. Muhlleitner and M. Spira, Phys. Rev. D **68**, 117701 (2003) [hep-ph/0305288].
- [8] E. J. Chun, K. Y. Lee and S. C. Park, Phys. Lett. B **566** (2003) 142 [hep-ph/0304069].

- [9] A. G. Akeroyd and M. Aoki, Phys. Rev. D **72** (2005) 035011 [hep-ph/0506176].
- [10] T. Han, B. Mukhopadhyaya, Z. Si and K. Wang, Phys. Rev. D **76** (2007) 075013 [arXiv:0706.0441 [hep-ph]].
- [11] J. Garayoa and T. Schwetz, JHEP **0803** (2008) 009 [arXiv:0712.1453 [hep-ph]].
- [12] M. Kadastik, M. Raidal and L. Rebane, Phys. Rev. D **77** (2008) 115023 [arXiv:0712.3912 [hep-ph]].
- [13] A. G. Akeroyd, M. Aoki and H. Sugiyama, Phys. Rev. D **77** (2008) 075010 [arXiv:0712.4019 [hep-ph]].
- [14] P. Fileviez Perez, T. Han, G. -y. Huang, T. Li and K. Wang, Phys. Rev. D **78** (2008) 015018 [arXiv:0805.3536 [hep-ph]].
- [15] F. del Aguila and J. A. Aguilar-Saavedra, Nucl. Phys. B **813**, 22 (2009) [arXiv:0808.2468 [hep-ph]].
- [16] A. G. Akeroyd, C. -W. Chiang and N. Gaur, JHEP **1011** (2010) 005 [arXiv:1009.2780 [hep-ph]].
- [17] A. G. Akeroyd and H. Sugiyama, Phys. Rev. D **84** (2011) 035010 [arXiv:1105.2209 [hep-ph]].
- [18] A. Melfo, M. Nemevsek, F. Nesti, G. Senjanovic and Y. Zhang, Phys. Rev. D **85** (2012) 055018 [arXiv:1108.4416 [hep-ph]].
- [19] M. Aoki, S. Kanemura and K. Yagyu, Phys. Rev. D **85** (2012) 055007 [arXiv:1110.4625 [hep-ph]].
- [20] A. G. Akeroyd, S. Moretti and H. Sugiyama, Phys. Rev. D **85** (2012) 055026 [arXiv:1201.5047 [hep-ph]].
- [21] B. Mukhopadhyaya and S. Mukhopadhyay, Phys. Rev. D **82** (2010) 031501 [arXiv:1005.3051 [hep-ph]]; Phys. Rev. D **84** (2011) 095001 [arXiv:1108.4921 [hep-ph]].
- [22] For a recent update, see, D. V. Forero, M. Tortola and J. W. F. Valle, arXiv:1205.4018 [hep-ph].
- [23] CMS Collaboration, CMS-PAS-HIG-12-005

- [24] J. Pumplin, A. Belyaev, J. Huston, D. Stump and W. K. Tung, JHEP **0602**, 032 (2006) [hep-ph/0512167].
- [25] A. Pukhov, hep-ph/0412191.
- [26] J. Alwall, A. Ballestrero, P. Bartalini, S. Belov, E. Boos, A. Buckley, J. M. Butterworth and L. Dudko *et al.*, Comput. Phys. Commun. **176**, 300 (2007) [hep-ph/0609017].
- [27] T. Sjostrand, S. Mrenna and P. Z. Skands, JHEP **0605**, 026 (2006) [hep-ph/0603175].